World Academy of Science, Engineering and Technology
International Journal of Bioengineering and Life Sciences
Vol:8, No:12, 2014

Synthesis of Novel Nanostructured Catalysts for Pyrolysis of Biomass

Phuong T. Dang, Hy G. Le, Giang T. Pham, Hong T. M. Vu, Kien T, Nguyen, Canh D. Dao, Giang H. Le, Hoa T. K. Tran, Quang K. Nguyen, Tuan A. Vu

Abstract**—**Nanostructured catalysts were successfully prepared by acidification of diatomite and regeneration of FCC spent catalysts. The obtained samples were characterized by IR, XRD, SEM, EDX, MAS-NMR (^{27}Al and ^{29}Si), NH_3-TPD and tested in catalytic pyrolysis of biomass (rice straw). The results showed that the similar bio-oil yield of 41.4% can be obtained by pyrolysis with catalysts at 450^{o}C as compared to that of the pyrolysis without catalyst at 550^{o}C. The bio-oil yield reached a maximum of 42.55% at the pyrolysis temperature of 500^{o}C with catalytic content of 20%. Moreover, by catalytic pyrolysis, bio-oil quality was better as reflected in higher ratio of H/C, lower ratio of O/C. This clearly indicated high application potential of these new nanostructured catalysts in the production of bio-oil with low oxygenated compounds.

Keywords**—**Acidified diatomite, biomass, catalytic pyrolysis, bio-oil, nanostructured catalysts, regenerated FCC catalyst.

I. Introduction

DUE to the limited availability of fossil feedstock, the manufacture of high value fuel products from low value feedstock like heavy oil residues, oil sands or biomass has received the great interest of researcher and oil producer. Rice straw is a biomass, which is abundant lignocellulose products from rice production in farming, but only a minor portion of these agricultural residues is reserved as animal feed, house hold fuel, or raw materials for paper industry. Huge quantities of the remaining rice straw are not used as industrial feed stock but being mainly burnt in the fields, causing significant environmental problems. For an agricultural country as Vietnam, rice straw is about 66% of total agricultural wastes. Annually, the total rice production in Vietnam is about 36-38 million tons which equals to about 65-69 million tons of rice straw [1]-[3]. Therefore, it can be recognized as a potential source for renewable energy based on benefits of both energy recovery and environmental protection. Lignocellulose is the main component of rice straw, which is a compact structure of cellulose (28-36%) and hemicellulose (23-28%) in close association with lignin (12-16%) [4].

Generally, biomass conversion processes can be divided in two main categories: biological (fermentation and anaerobic digestion) and thermochemical processes (combustion, gasification and pyrolysis). Among the various thermochemical conversion processes, pyrolysis is considered to be an emerging technology for converting biomass into fuel gases, liquids and solids, all of which can be used as an alternative fuel oil or chemical feedstock [5]-[8]. An addition, pyrolysis is attractive because solid biomass and wastes, which are difficult and costly to manage, can be readily converted to liquid products, bio-oils, that has many advantages in transport, storage, handling, retrofitting, combustion and flexibility in production and marketing [5], [7]. Biomass pyrolysis is a combustion in the absence of oxygen, or with a limited oxygen supply, to produce an oil-like liquid (named bio-oil or bio-liquid), a gas mixture containing mainly carbon oxides, some methane and higher gaseous hydrocarbon in minor quantities, and a solid residue rich in carbon. Among them, bio-oil is the most interesting product, which is a complex mixture of organic compounds and can be used as feedstock to produce bio-fuel by hydrodeoxygenation (HDO). Moreover, as-proceed bio-oil can be utilized as a source for valuable chemicals, such as phenols, after applying separation methods. It is also considered as a potential biofuel since it can be easily transported, be burned directly in thermal power station or in gas turbines, be utilized as a feedstock in a conventional petroleum refinery and be upgraded to obtain more valuable light hydrocarbon fuels [9], [10]. However, the high amount of water and oxygenates which reduce the calorific value of the bio-oil and change significantly its combustion characteristics. The presence of organic compounds with undesirable properties (organic acid, carbon), and of polycyclic aromatic hydrocarbons limits its potential for direct use in engines or turbines.

In order to improve the quality of the bio-oil produced as well as to optimize the conversion processes of biomass to fuels and chemicals, various catalysts have been introduced in pyrolysis. Zeolitic catalysts such as Y and ZSM-5 zeolites, FCC are used in biomass conversion and upgrading processes [11], [12].

Fluidized catalytic cracking (FCC) is one of the most important processes to produce gasoline and diesels. FCC catalysts consist of active components like zeolite Y, rare-earth modified zeolite-Y, USY and silica and/or aluminosilicates as supports. However, they suffer from large

Phuong T. Dang is with the Institute of Chemistry, VAST, 18 Hoang Quoc Viet, Cau Giay, Hanoi, Vietnam (corresponding author, phone: 84-4-38361145; fax: 84-4-38361283; e-mail: phuongdt@ich.vast.vn).

Hy G. Le is with the Center for High Technology Development, VAST, 18 Hoang Quoc Viet, Cau Giay, Hanoi, Vietnam (e-mail: legiahy@ibt.ac.vn).

Giang T. Pham, Kien T. Nguyen, Canh D. Dao, Giang H. Le, Hoa T. K. Tran, Quang K. Nguyen, and Tuan A. Vu are with the Institute of Chemistry, VAST, 18 Hoang Quoc Viet, Cau Giay, Hanoi, Vietnam (e-mail: phamthugiang78@gmail.com, kienvandinh@gmail.com, duccanh2812@gmail.com, giangnasa86@gmail.com, hoatra63@gmail.com, quangnguyenke89@gmail.com, vuanhtuan.vast@gmail.com)

Hong T. M. Vu is with the Hanoi University of Mining and Geology, Dong Ngac, Tu Liem, Hanoi, Vietnam (e-mail: vhongsla07@gmail.com).

crystal size (1-5μm) and narrow pore dimension (0.74 nm for zeolite Y) limiting the access of active sites by large molecules such as polyaromatics, lignocellulose. Improvement of catalytic performance and considering sustainability aspects needs the development of new generation of FCC catalysts. These catalysts should possess multi-modal pore structures of interconnected macro – meso - and micropores. They should allow easy access of heavy feedstock compartments to catalyst active sites. In this way, large polyaromatics can be pre-cracked in the mesopores. Further cracking at acidic sites in the micropores converts the pre-cracked compounds into valuable fuel components and other valuable chemicals [13]-[17]. Furthermore, the catalyst supports are usually inactive, so it needs the activation by acidification to improve the catalytic performance by synergetic effects between the active components and supports [18]-[26].

Diatomaceous earth, or diatomite, is a material of sedimentary origin consisting mainly of an accumulation of skeletons formed as a protective covering by diatoms. The structure of diatomite is quite complex and contains macropores, cavities and channels, and therefore the material has a high absorption capacity and low density. Other intrinsic properties are low thermal conductivity, relatively high melting-point, chemical inertness and small grain size [27]. Generally, diatomite has poor chemical activity; the incorporation of aluminum into porous silica framework of diatomite can form acid sites, which will greatly increase their catalytic applications [28]. Acid activation of clay minerals is one of the most effective methods that are used to produce active materials for adsorption and catalysis purposes. One of the most effective methods to acidify diatomite or pure silica frameworks is to apply the "Atomic Implantation" method to incorporate aluminum into frameworks by evaporating aluminum halides ($AlCl_3$) at high temperature (500-550^{o}C) [29].

A combination between the acidified porous materials and regenerated FCC catalysts would be a new alternative to produce highly active catalytic materials. These materials were expected to enhance the cracking activity of the big lignocellulosic molecules and to produce a liquid product with less oxygenated compounds and possibly richer in high-value products.

In this paper, we report the recent results on the acidification of diatomite (Phu Yen - Vietnam) by aluminum atomic implantation and the preparation of new nanostructured catalyst based on the acidified diatomite and the regenerated FCC for pyrolysis of rice straw.

II. Experimental

A. Rice Straw Composition

Rice straw samples used in this study were taken from a farm in Northern Vietnam. These samples were dried in the sunshine to remove most of moistures, washed by water for separating physical impurities such as sand and fire fractions, and then further dried at 100^{o}C for 24h. Finally, the samples were cut into small fractions with particle diameter of 0.3-0.5 mm.

A complete compositional analysis was performed on the rice straw samples that were used as feedstock for bio-oil production. This analysis included chemical composition as well as elemental and proximate analysis. Chemical composition was determined using TAPPI standard method. Elemental (ultimate) analysis was performed on a Flash EA 1112 element analyzer. Proximate analysis was carried out for moisture, combustible content and ash. Heating values of rice straw and bio-oil was determined using ASTM D 240-00 on Parr Calorimeter 6200. The moisture was obtained from the difference between the original mass and the mass after drying for 2h at 100±5^{o}C. The combustible content was measured from the difference between the mass dried for 2h at 100±5^{o}C and the final mass burned for 3h at 800±5^{o}C. The final mass was the ash. Composition of rice straw was listed in Table I. In Table I, the combustible matter of rice straw was 80.16 wt %, supporting the use of rice straw as an energy source. The content of C and O were 53.94 and 39.2%, respectively. It was obvious that sulfur and nitrogen was rare. The obtained results supported that rice straw have a potential advantage in the application of biomass for energy and is alternative and chemical resources produced from pyrolysis.

TABLE I
Characteristics of the Rice Straw

Proximate analysis (wt %)		Component analysis (wt %)		Ultimate analysis (wt %)[a]	
Moisture	7.08	Cellulose	60.62	Carbon	53.94
Combustible	80.16	Hemicellulose	25.64	Hydrogen	5.84
Ash	12.76	Lignin	15.74	Nitrogen	1.02
				Oxygen[b]	39.20
				Sulfur	0.02

[a] Dry-ash-free basic
[b] By difference

B. Preparation and Characterization of Catalysts

The Diatomite support (Phu Yen-Vietnam) was calcined at 500°C, treated with HCl 1M under reflux. Acidification of diatomite was carried out as follows: Purified diatomite and aluminum chloride in excess, separated by a quartz filter, were placed into a tubular reactor. The reactor was heated to the final temperature of up to 500°C. The $AlCl_3$ was evaporated through the diatomite with nitrogen carrier gas (N_2). Regeneration of waste catalyst from RFCC unit of Dung Quat refinery were carried out by coke burning at 650^{o}C for 6 hours and washing with oxalic acid of 1M concentration for 3h. New catalysts were a mixture of 80% (wt.) regenerated FCC and 20% (wt.) acidified diatomite.

Low-angle X-ray diffraction patterns were obtained on a Bruker D8 Advance instrument using CuK_α radiation with generator operated at 40 KV and 40 mA, the patterns were recorded at room temperature (298 K), scanning angle 2θ was 0.5-15^o, the scanning step was 0.03^o, and step time was 0.3s. The IR spectra of rice straw were recorded from disk-membrane samples (1%) in KBr pellets by Impact–410 IR spectra photometer. Nitrogen adsorption/desorption isotherms at 77K were established using an Omnisorp-100 apparatus.

The specific surface area, SBET, was determined from the BET equation. The mesopore size distribution was determined from the desorption branch of the N_2 adsorption/desorption isotherms using the Barrett-Joyner-Halenda (BJH) formula. Scanning electron microscopy (SEM) images were obtained on a JSM-5300 LV. Temperature programmed desorption (TPD-NH_3) measurements were carried out on an Autochem II 2920 apparatus in a flow reactor. Samples were activated at 700°C for 1h in a flow of helium. Subsequently, ammonia was introduced by a helium stream containing 10 % (vol.) ammonia at 100°C. The physically adsorbed NH_3 was removed by purging with a He flow at 100°C until the baseline was flat. Then the reactor temperature was ramped at a rate of 10°C/min.

C. Pyrolysis Experiments

Pyrolysis experiments were performed in a 316 stainless steel fixed-bed tubular reactor (3.67cm internal diameter and 60 cm long). It is externally heated by an electrical furnace and the temperature measured by thermocouple inside the bed. For all experiments, the mass (~5g, in each experiment) of sample placed on the top of the catalyst bed and amount of catalyst (10, 20, 30 wt. %) or glass beads for the non-catalytic tests were placed inside the reactor. The sweep gas from a nitrogen cylinder was dried and purified by a molecular sieve tube. The experimental conditions in the pyrolysis system were as the following: pyrolysis temperature of 450°C-550°C, sweep gas flow rate of 160ml/min. Solid product (char) was removed and weighed after the experiment. The liquid phase was collected in a cold trap maintained at about 0°C using salty ice as cooling agent. The liquid phase consisted of aqueous and oil phase which were separated by dichloromethane and weighed. The yield of the resulting products was thus calculated based on the mass of the sample feed. The gas yield was obtained by making difference between the sum of products and liquid-char.

III. Results and Discussion

A. Characterization Catalysts

* FCC Samples

Fig. 1 showed FTIR spectra of spent and regenerated FCC. As seen in Fig. 1, the band at ~2950cm^{-1} is assigned to C-H bonding which disappeared after regeneration (coke burning and acid treatment). This revealed that coke was removed.

The crystallinty of spent and regenerated FCC catalyst has been examined by XRD (Fig. 2). The XRD patterns of both these samples were the same and showed the regeneration of spent FCC catalyst by combination of coke burning and acid treatment still maintained the structure.

In the NH_3–TPD profiles of the regenerated FCC samples (Fig. 3), two peaks: a low temperature peak (150°C-250°C) and a high temperature peak (400°C-550°C) corresponding to weak and strong acid sites were observed. While in NH_3 TPD profile of spent FCC, a large amount of weak acid sites desorbing ammonia at 200°C (maximum) was noted. A small amount of strong acid sites (maximum temperature of 530°C) was observed. Nitrogen adsorption–desorption isotherms and the pore size distribution of regenerated FCC were presented in the Fig. 4. In Fig. 4 as can be seen, the isotherms of regenerated FCC are classified as type IV with the hysteresis loops, which were typical for mesoporous materials. The total specific surface area and the pore diameter of regenerated FCC are 168.82 m²/g and 9.2 nm, respectively.

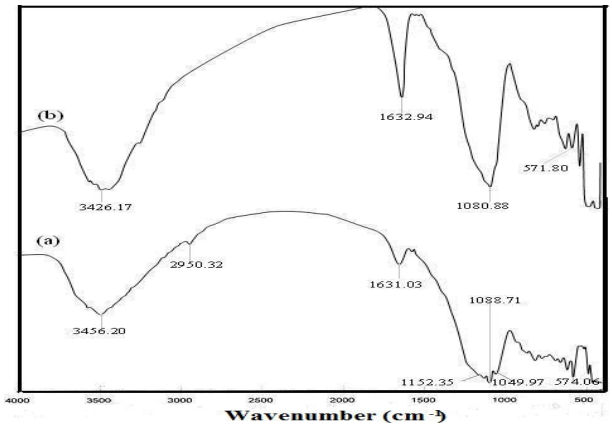

Fig. 1 IR spectra of spent (a) and regenerated (b) FCC

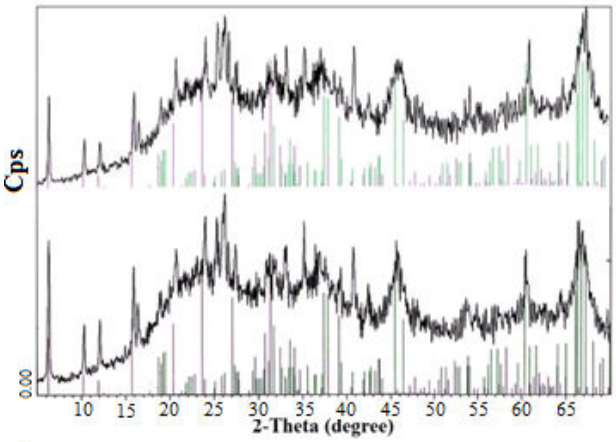

Fig. 2 XRD patterns of spent (a) and regenerated (b) FCC

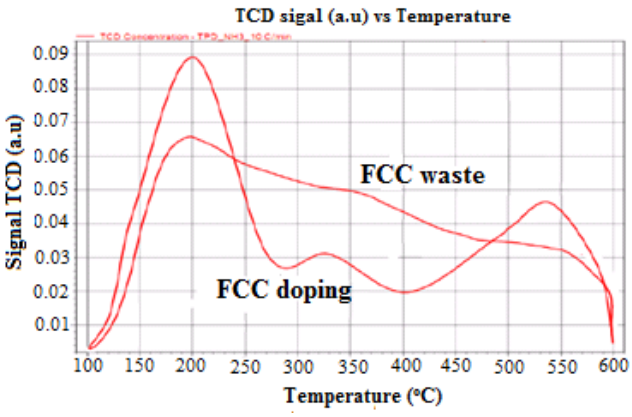

Fig. 3 NH_3-TPD profiles of spent and regenerated FCC

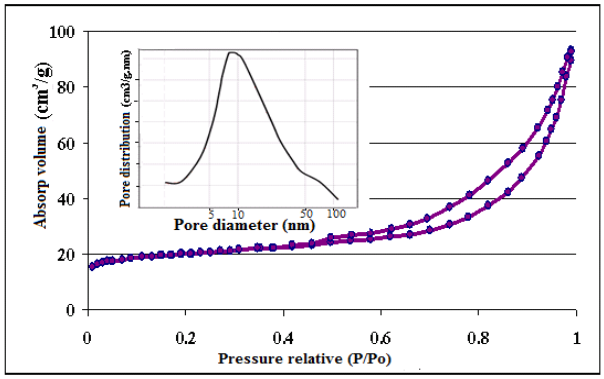

Fig. 4 Nitrogen adsorption - desorption isotherms and the pore size distributions of regenerated FCC

* Diatomite

Element compositions of raw diatomite and acidified diatomite determined by EDX analysis data were given in Table II. It was noted that aluminum content increased from 6.34 wt. % to 8.21 wt. %, indicating the insertion of aluminum into diatomite framework.

TABLE II
ELEMENT COMPOSITION OF RAW DIATOMITE AND ACIDIFIED DIATOMITE

Elemental analysis (wt %)	Raw diatomite	Acidified diatomite
O	54.07	53.41
Mg	0.33	0.26
Al	6.34	8.21
Si	33.53	32.50
Ti	0.84	0.74
Fe	4.89	4.88
Sum	100	100

SEM images of diatomite and acidified diatomite were illustrated in Fig. 5. As can be seen, acidified diatomite had the macro-meso structure with the typically cylindrical shape (Fig. 5 (A)). The SEM images showed this sample consisted of cylindrical tubes with diameter of 8-10 µm, length of 10 -20 µm and on their surface existed regular arrays of pores with a diameter of 0,5-0,8 µm. It showed that, the acidification of diatomite still maintained the structure of diatomite (Fig. 5 (B)).

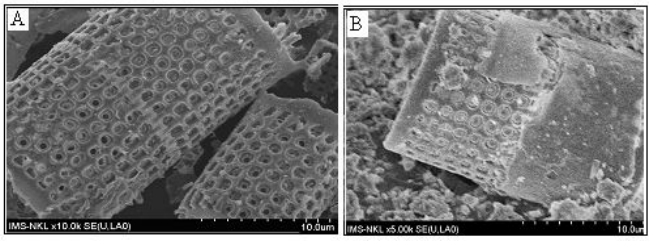

Fig. 5 SEM images of acidified diatomite (A) and diatomite samples (B)

Nitrogen adsorption–desorption isotherms and the pore size distribution of acidified diatomite and diatomite, were presented in the Fig. 6. As observed, the isotherms of acidified diatomite and diatomite are classified as type IV with the hysteresis loops, which were typical for mesoporous materials. The total specific surface area calculated by BET method is 41.5 m^2/g. As can be seen in Fig. 6, the pore diameter of the acidified diatomite was 9.2 nm.

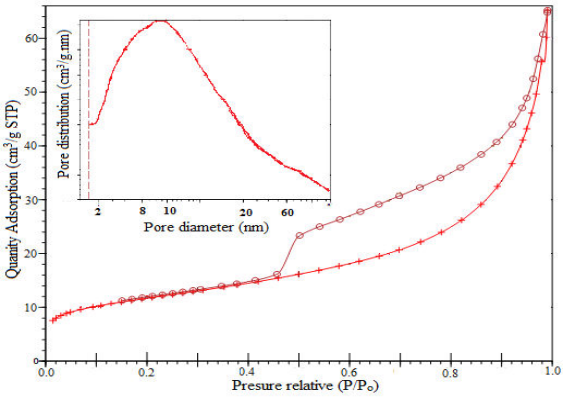

Fig. 6 Nitrogen adsorption - desorption isotherms and the pore size distributions of acidified diatomite

^{27}Al and ^{29}Si magic angle spinning NMR has been proven to be a very informative technique for structural studies of silicates and aluminosilicates, for a deeper understanding of their structural properties [30]. ^{27}Al MAS-NMR can provide information for different oxygen coordination around the Al atom. ^{29}Si MAS-NMR is capable of distinguishing SiO_4 tetrahedral of connectivity ranging from 0 to 4, represented by the symbol Qm, where m is the number of bridging oxygen. ^{29}Si MAS-NMR is able of distinguishing different cross-linked Si tetrahedral and is a very sensitive technique for determination of the substitution of Al for Si tetrahedral by the characteristic ^{29}Si line shifts.

Fig. 7 (A) presented the ^{27}Al- MAS-NMR spectra of raw and acidified diatomite. For raw diatomite sample, in the ^{27}Al-NMR spectrum appeared two main resonance peaks at 0 ppm and 58 ppm. For acidified diatomite sample, in the ^{27}Al-NMR spectrum appeared two main resonance peaks at 10 ppm and 58 ppm. ^{27}Al resonance peak at 0 ppm is assigned to the hydroxylated aluminum octahedral layers [10]. ^{27}Al resonance peak at 10 ppm is attributed to the octahedral aluminum sites where the resonance peak at 58 ppm is assigned to the tetrahedral aluminum sites [31]-[34].

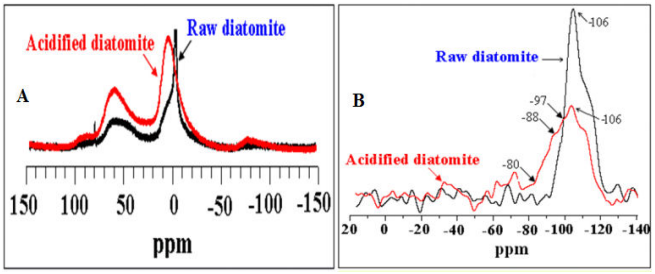

Fig. 7 ^{27}Al MAS NMR (A) and ^{29}Si-MAS NMR (B) spectra of the raw diatomite and acidified diatomite

As can be seen in Fig. 7 (A), much higher peak intensity at 58 ppm observed on the acidified diatomite as compared to

that of raw diatomite, indicating the enhance of tetrahedral Al sites of the diatomite sample after Al substitution for Si into silicate framework.

Fig. 7 (B) illustrated the ^{29}Si MAS-NMR spectra of raw diatomite and acidified diatomite. In the ^{29}Si-NMR spectrum of raw diatomite, a sharp resonance peak centered at -106 ppm was observed. In contrast, in the ^{29}Si-NMR spectrum of acidified diatomite, a broadness of the resonance peak at -106 ppm and shoulders at -97, -88 and -80 ppm were noted. This broadness is due to a range of Si-O-T (T= Si or Al) bond angles with Si-O sheet networks remain unchanged, the major change being a flattening of Si-O linked to Al sheet [32]. The observed down field ^{29}Si chemical shifts are may be due to the aluminum substitution in silicate units. It is well documented in the literature [31]-[33], the resonance peaks at -80, -88, -97 and -106 ppm are indicative for the formation of substituted Q1, Q2, Q3 and Q4 structural units by reaction between aluminum sites and Q4 silicate units. The presence of resonance peak as shoulder at -80, -88, -97 ppm in the ^{29}Si-NMR spectrum of the acidified diatomite sample gives evidence for Al insertion into diatomite framework. Combination of ^{27}Al and ^{29}Si-MAS-NMR results, it is clearly indicated that after acidification, aluminum is really incorporated into diatomite framework.

Fig. 8 presented the NH_3-TPD profiles of raw and acidified diatomite. The NH_3-TPD profiles of both raw and acidified diatomite samples showed the two main peaks: low temperature peak at 180-200^{o}C and high temperature peak at 450-470^{o}C. However, for raw diatomite sample, low temperature peak is predominant, whereas for acidified diatomite sample, high temperature peak is predominant.

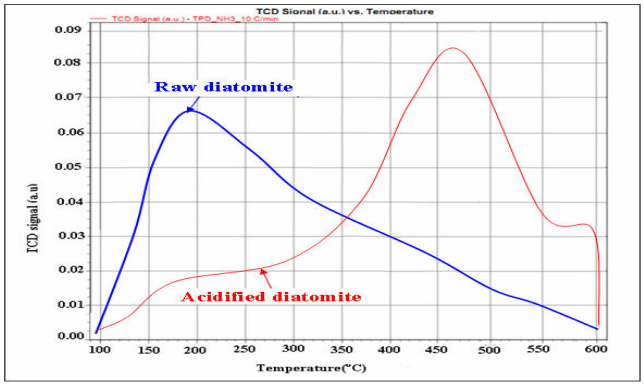

Fig. 8 NH_3-TPD profiles of raw diatomite NH_3 and acidified diatomite samples

B. Catalytic Activity

Product yield from pyrolysis was indicated in the (Table III). In the presence of catalyst, the yield of liquid product increase from 40.78% to 42.55% with increasing of content of catalyst from 10% to 20%. The increase in liquid products could be mainly attributed to the secondary cracking of pyrolysis vapor products on acid sites of catalyst. Furthermore, the increasing of content of catalyst to 30% will reduce the liquid product by 35.72%. The secondary decomposition of organic compounds may also give non-condensable gaseous products which would lead to the increase in gas yield in presence of catalyst. The liquid yield reached a maximum of 42.55% at the pyrolysis temperature of 450^{o}C in presence of 20% catalyst amount of feedstock.

The obtained results showed that the similar liquid product of ~41% can be reached by pyrolysis with catalysts (10%) at 450^{o}C as compared to that of the pyrolysis without catalyst at 550^{o}C (Table III).

The liquid fraction of the pyrolysis products consists of two phases: an aqueous phase containing a wide variety of organic-oxygenated compounds (water and water soluble organic compounds) with low molecular weight, and a non-aqueous phase containing insoluble organics (oil) with high molecular weight. It is well known, rice straw has low heating value in actual applications. The rice straw pyrolysis can produce the bio oil with higher heating value (Table IV).

TABLE III
PRODUCT YIELD FROM PYROLYSIS

Content of catalyst (wt %)	Pyrolysis temperature (^{o}C)	Liquid (wt %)	Gas (wt %)	Solid (wt %)
10	450	40.78	27.34	31.88
20	450	42.55	28.70	38.75
30	450	35.72	35.54	28.74
0	550	40.69	25.49	33.82

From the Table IV, it showed the heating value of liquid products (non-aqueous phase) in catalytic pyrolysis is higher than ~1.8 times compared to that of rice straw and ~ 1.6 times compared with when no using catalyst. This strongly suggests that heating value depends on chemical composition of products. It is well documented that the products contain more paraffinic hydrocarbon and less oxygen-containing compounds possessing higher heating value.

TABLE IV
HEATING VALUE OF RICE STRAW AND LIQUID PRODUCTS (NON-AQUEOUS PHASE) AT THE PYROLYSIS TEMPERATURE OF 450^{o}C

Samples	Heating value
Rice straw	14.64 MJ/kg
Liquid products (non-aqueous phase) without catalysts	17.46 MJ/kg
Liquid (non-aqueous phase) with catalysts	27.23 MJ/kg

TABLE V
ELEMENT COMPOSITION (WT. %)

Elements	Rice straw	Liquid products (non-aqueous phase) without catalysts	Liquid (non-aqueous phase) with catalysts
C	53.94	67.01	68.31
H	5.84	7.94	8.09
N	1.02	1.66	1.94
O	39.20	23.39	21.66
H/C	1.29	1.39	1.42
O/C	0.54	0.26	0.22

The elemental compositions (C, H, N, O) in the products are presented in Table V. Ratio H/C in products when using higher catalyst compared with the non-catalytic one, led to the higher value of the product. These results are in agreement with the heating value data. In contrast, the ratio O/C is lower observed in the case of pyrolysis with catalysts. Additionally,

comparing to the thermal pyrolysis, catalytic pyrolysis produces more phenols and less oxygenate compounds. Pyrolysis oil may be used either as a fuel or as a source of valuable chemicals.

IV. Conclusion

New nanostructured catalysts were successfully prepared by using the acidified diatomite and the modified FCC catalysts, which were regenerated by the combination of coke burning and acid treatment of spent FCC catalyst from Dung Quat refinery. In the presence of these new nanostructured catalysts, the liquid yield reached a maximum of 42.55 wt.% at the pyrolysis temperature of 450^{o}C with catalyst content of 20 wt.%. The similarly liquid yield of 41.4 wt.% can be reached by pyrolysis with catalysts (10 wt.%) at 450^{o}C as compared to that of the pyrolysis without catalyst at 550^{o}C. Moreover, by catalytic pyrolysis, bio-oil quality was better as reflected in higher ratio of H/C and lower ratio of O/C. This clearly indicated high application potential of these new nanostructured catalysts in the production of bio-oil with low oxygenated compounds.

Acknowledgment

The authors acknowledge the National Foundation for Science and Technology Development of Vietnam - NAFOSTED (Grant no. 104.03-2012.34) for financial support.

References

[1] N. W. A. Lindula, N. Mithulananthan, X. Ongsakul, C. Widjaya, R. Henson, "ASEAN towards clean and sustainable: Potentials, utilization and berries", *Renewable Energy*, vol. 32, 2007, pp. 1441-1454.

[2] Truong Nam Hai, "Current status of biomass utilization in Viet Nam", *Biomass-Asia Workshop*, 2005.

[3] Tran Huu Thuc, "General statistic office, Statistical yearbook of Vietnam", Statistical Publishing House, 2006.

[4] R. C. Sun, J. Tonkinson, F. C. Mao, "Physicochemical characterization of lignin from rice straw by hydrogen peroxide treatment", *J. Appl. Polym. Sci.*, vol. 79, 2001, pp. 719-932.

[5] A. V. Bridgenater, G. Grassi, "Biomass pyrolysis liquids upgrading and utilization", England, Elservier Applied Science, 1991.

[6] R. F. Probstein, R. E. Hicks, "Synthetic fuels", McGraw-Hill Book Company, New York, 1982.

[7] J. M. Encina, J. F. Gonzalez, J. Gonzalez, "Fixed-bed pyrolysis of cynara cardunculus. Product and composition", *Fuel Processing Technology*, vol. 63, 2000, pp. 209-222.

[8] P. McKendry, "Energy production from biomass (part 2): Conversion technologies", *Bioresour. Technol.*, vol. 83, 2002, pp. 47-54.

[9] M. N. Islam, M. R. A. Beg, "The fuel properties of pyrolysis liquid derived from urban solid wastes in Bangladesh", *Bioresour. Technol*., vol. 92, 2004, pp. 181-186.

[10] G. W. Huber, J. A. Dumesic, "An overview of aqueous-phase catalytic processes for production of hydrogen and alkanes in a biorefinery", *Catal. Today*, vol. 111, 2006, pp. 119-132.

[11] P. T. Williams, N. Nugranad, "Comparison of products from the pyrolysis and catalytic pyrolysis of rice husks", *Energy*, vol. 25, 2000, pp. 493-513.

[12] E. M. Sulman, V. V. Alferov, Yu. Kosivtsov, A. I. Sidorov, O. S. Misnikov, A.E. Afanasiev, N. Kumar, D. Kubicka, J. Agullo, T. Salmi, D.Yu. Murzin, "The development of method of low-temperature peat pyrolysis on the basis of aluminosilicate catalytic system", *Chem. Eng. J*., vol. 134, 2007, pp. 162-167.

[13] Y. Liu, W. Zhang, T.J. Pinnavaia, "Steam-stable aluminosilicate mesostructures assembled from zeolite type Y seeds", *J. Am. Chem. Soc.*, 122 (2000) 8791.

[14] Y. Liu, W Zhang, T. J. Pinnavaia, Steam-stable MSU-S aluminosilicate mesostructures assembled from zeolite ZSM-5 and zeolite Beta seeds, Angew. *Chem. Int*. Ed., vol. 40, 2001, pp. 1255.

[15] K. S. Triantaflyllidis, T. J. Pinnavaia, A. Iosifidis, P. J. Pomonis, "Specific surface area and I-Point evidence for microporosity in nanostructure MSU-S aluminosilicates assembled from zeolite seeds", *Journal of Mater. Chem*., vol. 17, 2007, pp. 3630.

[16] Z. Jing, Hirotaka, K. Ioku, E. H. Ishida, "Hydrothermal Synthesis of Mesoporous Materials from Diatomaceous Earth", J. *AIChE*, vol. 53, 2007, pp. 2114.

[17] S. W. Rutherford, J.E. Coons, "Water sorption in silicone foam containing diatomaceous", *J. Colloid Interface Sci*, vol. 306, 2007, pp. 228.

[18] Min Lu, Pengmei Lv, Zhenhong Yuan, Huiwen Li, "The study of bimetallic Ni–Co/cordierite catalyst for cracking of tar from biomass pyrolysis", *Renewable Energy,* vol. 60, December 2013, pp. 522-528.

[19] Shuai Leng, Xinde Wang, Xiaobo He, Lin Liu, Yue'e Liu, Xing Zhong, Guilin Zhuang, Jian-guo Wang, "NiFe/γ-Al2O3: A universal catalyst for the hydrodeoxygenation of bio-oil and its model compounds", *Catalysis Communications*, vol. 41, 5 November 2013, pp. 34-37.

[20] Xun Hu, Caroline Lievens, Daniel Mourant, Yi Wang, Liping Wu, Richard Gunawan, Yao Song, Chun-Zhu Li, "Investigation of deactivation mechanisms of a solid acid catalyst during esterification of the bio-oils from mallee biomass", *Applied Energy*, vol. 111, November 2013, pp. 94-103.

[21] Sikander H. Hakim, Brent H. Shanks, James A. Dumesic, "Catalytic upgrading of the light fraction of a simulated bio-oil over CeZrOx catalyst", Applied Catalysis B: Environmental, vol. 142–143, October–November 2013, pp. 368-376.

[22] Sudhagar Mani, James R. Kastner, Ankita Juneja, "Catalytic decomposition of toluene using a biomass derived catalyst", *Fuel Processing Technology,* vol. 114, October 2013, pp. 118-125.

[23] Ferenc Lónyi, József Valyon, Edward Someus, Jenő Hancsók, "Steam reforming of bio-oil from pyrolysis of MBM over particulate and monolith supported Ni/γ-Al2O3 catalysts", *Fuel*, vol. 112, October 2013, pp. 23-30.

[24] Lei Wang, Dalin Li, Mitsuru Koike, Hideo Watanabe, Ya Xu, Yoshinao Nakagawa, Keiichi Tomishige, "Catalytic performance and characterization of Ni–Co catalysts for the steam reforming of biomass tar to synthesis gas", *Fuel,* vol. 112, October 2013, pp. 654-661.

[25] Xiwei Xu, Enchen Jiang, Bosong Li, Mingfeng Wang, Gang Wang, Qian Ma, Dongdong Shi, Xinhui Guo, "Hydrogen production from wood vinegar of camellia oleifera shell by Ni/M/γ-Al2O3 catalyst", *Catalysis Communications*, vol. 39, 5 September 2013, pp. 106-114.

[26] C. E. Greenhalf, D. J. Nowakowski, N. Yates, I. Shield, A. V. Bridgwater, "The influence of harvest and storage on the properties of and fast pyrolysis products from Miscanthus x giganteus", *Biomass and Bioenergy*, vol. 56, September 2013, pp. 247-259.

[27] K. Chaiwong, T. Kiatsiriroat, N. Vorayos, C. Thararax, "Study of bio-oil and bio-char production from algae by slow pyrolysis", *Biomass and Bioenergy*, vol. 56, September 2013, pp. 600-606.

[28] Osman Şan, Remzi Gören, Cem Özgür, "Purification of diatomite powder by acid leaching for use in fabrication of porous ceramics", *Int. J. Miner. Process*, vol. 93, 2009, pp. 6–10.

[29] Chun Hui Zhou, "Clay Mineral-based Catalysts and Catalysis", *Applied Clay Science,* vol. 53, 2011, pp. 87–96.

[30] C. D. Chang, C. T-W. Chu, J. N. Miale, R. F. Bridger, R. B. Calvert, "Aluminum insertion into high silica zeolite frameworks. 1. Reaction with aluminum halides", *J. Am. Chem. Soc*., vol. 106, 1984, pp. 8143-8146.

[31] G. Engelhardt and D. Michel, "High-Resolution Solid-State NMR of Silicates and Zeolites", John Wiley & Sons Ltd., 1987.

[32] V. F. F. Barbosa, K. J. D. Machenzie and C. Thaumaturgo, "Synthesis and characterisation of materials based on inorganic polymers of alumina and silica: sodium polysialate polymers", *Int. J. Inog. Mater*., vol. 2, 2000, pp. 309.

[33] K. J. D. Mackenzie, I. W. M. Brown, R. H. Meinhold, M. E. Bowden, "Outstanding Problems in the Kaolinite-Mullite Reaction Sequence Investigated by 29Si and 27Al Solid-State Nuclear Magnetic Resonance: I. Metakaolinite," J. Am. Ceram. Soc., vol. 68, 1985, pp. 293-297.

[34] P. S. Singh, Tim Bastow, Mark Trigg, "Structural studies of Geopolymers by 29Si and 27Al MAS-NMR", *Journal of Materials Science*, vol. 40, 2005, p. 3951.